Atmospheric Pollution Research 13 (2022) 101488

Contents lists available at ScienceDirect

Atmospheric Pollution Research

journal homepage: www.elsevier.com/locate/apr

Outdoor and indoor measurements of number particles size distributions and equivalent black carbon (EBC) at a mechanical manufacturing plant

Giulia Pavese [a,*], Francesca Agresti [a,b], Mariarosaria Calvello [a], Francesco Esposito [b], Antonio Lettino [a]

[a] Consiglio Nazionale delle Ricerche- Istituto di Methodologies per l'Analisi Ambientale (CNR- IMAA), C. da S. Loja, 85050, Tito Scalo, Potenza, Italy
[b] Università della Basilicata - Scuola di Ingegneria, C. da Macchia Romana, 85100, Potenza, Italy

ARTICLE INFO

Keywords:
Mechanical manufacturing plant
Indoor/outdoor measurements
Equivalent black carbon
Number particle size distribution

ABSTRACT

Human exposure to air pollution is of great concern, especially in working places, where many people spend a lot of time. This work describes results obtained during a measurements campaign (February–July 2021) of aerosol number size distributions and equivalent black carbon (EBC), inside and outside a mechanical manufacturing plant, in Southern Italy. Outdoor and indoor EBC data are highly correlated ($R^2 = 0.98$) suggesting the same sources: vehicular traffic, domestic heating and agricultural waste burning (February–April). In these months the outdoor Angstrom absorption exponent (AAE) was highly oscillating (0.64–1.62), with reduced oscillations (0.9–1.5) during warmer months. These last values suggest the influence of a diffuse cloud of aged smoke due to uncontrolled and extended wheat biomass burning, lasting about one month, in the nearby Apulia region. A good correlation between outdoor EBC and NC1 (particles number with $D \leq 1$ μm) confirms that EBC has a high contribution to the aerosol size distribution. The same profile of number size distributions in both configurations indicates the same sources but, during cold months, the outdoor ones are characterized by higher values than the warm months, especially in the fine particles range. During working and non-working days, a reduction of indoor particles number concentration over the whole size range is observed throughout the weekend, suggesting manufacturing activities as one of the sources. Scanning electron microscope (SEM) analysis of outdoor and indoor spare internal filters shows the presence of metal particles indicating inside particles are being transported outside.

1. Introduction

Worldwide humans are exposed to pollution related to their activities, with detrimental effects to their health. The World Health Organization (WHO) estimates about seven million deaths every year due to air pollution, with 99% of persons breathing air that exceeds limits fixed by WHO itself (https://www.who.int/health-topics/air-pollution#tab=tab_1). Vehicular traffic, domestic heating, incinerators and manufacturing plants are the main pollution sources, with emissions of gases and particulate matter (PM). Focusing on particles emissions, sources such as incinerators (Moon et al., 2008; Jones and Harrison, 2016) and biomass burning for domestic heating (Küpper et al., 2018), are responsible of ultrafine and carbonaceous particles emissions, produced by incomplete combustion processes. Vehicular traffic is responsible for both black carbon (BC) and road-dust particles release, caused by the abrasion of brakes and by rotating wheels on the road. Considering manufacturing plants, polluting particles properties emitted during the activities are strictly related to the specific productions. In an interesting paper, Ehlrich et al.,2007 measured PM_{10}, $PM_{2.5}$ and $PM_{1.0}$ close to many industrial plants in different regions of Germany, to determine the dust fraction in the waste gases. The most relevant result was that mass particles size distributions were strictly related to specific industrial processes. Other studies report results on $PM_{2.5}$ emissions close to productive areas, but with scarce consideration of particulate speciation or size distributions, with an exception for 3D additive manufacturing (AM) activities, that are even more diffused. Chen et al. (2020) in a review discussed health issues of metal particles during AM production, identifying exposure paths, adverse human health effects and influencing factors that regulate PM toxicity. Stefaniak et al. (2021) analyzed forty-six articles describing all AM production processes,

Peer review under responsibility of Turkish National Committee for Air Pollution Research and Control.
* Corresponding author.
E-mail address: giulia.pavese@imaa.cnr.it (G. Pavese).

https://doi.org/10.1016/j.apr.2022.101488
Received 8 February 2022; Received in revised form 21 June 2022; Accepted 22 June 2022
Available online 28 June 2022

highlighting fine and ultrafine particles emission with specific compositional characteristics, dependent on the single process phase. Bhanarkar et al. (2010) studied gaseous and particulate matter emissions (unspecified dimensional fractions) from different operations in an integrated steel-pipe manufacturing plant in India and they found the highest PM emissions from the barrel grinding operation. Noth et al. (2014) measured total particulate matter (TPM) and $PM_{2.5}$ to evaluate the exposure in different facilities of an aluminum industry in the USA, and they observed higher TPM concentrations in smelters area than in other units. Indoor air quality, including work places, is affected also by outdoor sources, as discussed by Leung (2015). In its review, he examined the pathways followed by outdoor pollutants (gases and particles) to influence indoor environments. One of the outdoor pollutants affecting the indoor air quality is black carbon (BC). The relationship between outdoor and indoor pollutants was studied by Thatcher et al. (2014) in four distinct homes in an area (Cambria, USA) where the main BC source was domestic heating. Authors found a ratio BC_{in}/BC_{out} 0.78 $\pm$ 0.21 highlighting, the persistence of wood smoke particles in the indoor environment. On the other side, Tunno et al. (2015) evaluated the effect of outdoor $PM_{2.5}$ and BC in private homes located in an industrialized area near Pittsburgh (USA), and the higher indoor pollutants concentrations suggested smoking as an important source, especially for $PM_{2.5}$. Cartechini et al. (2015) measured number size distributions and BC concentration in an Italian museum during three measurement campaigns, each lasting one-week. The real-time data were integrated with a SEM and chemical analysis techniques. Nezis et al. (2022) studied the association between $PM_{2.5}$ and BC measured in a three-months campaign, with the sick building syndrome (SBS) described by employees of a public office in Athens. In another review, Riffault et al. (2015) examined morphology, size distributions and chemical composition of $PM_{2.5}$ close to different industrial activities, underlying the lack of a specific regulation for outdoor industrial environments, unlike the occupational standards adopted for indoor air in workplaces. Studying aerosol morphology and composition in indoor environments by SEM, specifically in work environments, is not common because of its poor cost-effectiveness. However, SEM allows obtaining very accurate information on particles dimensions, morphology, chemical composition and, eventually, mixing state. In order to establish a correlation between PM concentrations and human PM exposure, Conner et al. (2001) measured personal, indoor and outdoor PM concentrations in a retirement center in Baltimore (USA). They used a computer-controlled scanning electron microscope (CCSEM) with X-ray analysis on single particles to retrieve PM chemical and morphological characteristic in and around the retirement home and they recognized a key role of this technique to discriminate among particles having same composition; however, different morphology revealed different sources. Singh et al. (2017) looked for a relationship between air pollutants and physiological profiles of indoor kitchen workers with microalbuminuria (MAU) in north and south India. To this end they studied size and morphology of PM in indoor air by a SEM. The present study aims at characterizing aerosol particles at a mechanical manufacturing plant, both indoor and outdoor by measuring number particles size distributions by means of an Optical Particle Sizer (OPS) and equivalent black carbon (EBC) concentrations by means of an aethalometer. The indoor relevant source is represented by the handwork of metal hydraulics components produced by Computerized Numerical Control (CNC) machines, and manually refined afterward. To complete the particle characterization both outdoor and indoor, the OPS internal filter was analyzed by means of a SEM, highlighting the presence of particles derived by manufacturing operations, both indoor and outdoor. The measurements design has been useful also to evaluate the influence of outdoor sources on the indoor environment and vice-versa.

2. Site description

Measurements of number size distributions and EBC concentrations were performed at Pintotecno s.r.l. (https://www.pintotecno.com/), a mechanical manufacturing plant where metallic (aluminium, steel, cast iron) hydraulic components are produced either from bars or castings. The plant is a warehouse of 1200 m^2 located in Basilicata region, Southern Italy (40.93° N, 15.74° E). The area is a rural one, on the top of a hill (620 m a.s.l.), surrounded, within a radius of 7 km, by some towns uphill at heights varying between 415 m a.s.l. and 676 m a.s.l. with number of inhabitants ranging from 700 to 13,000. This area also hosts a cement plant and it is crossed by the road SP10, running very close to the measurement site.

This place is in the center of Vulture region, where the caldera of an extinct volcano gave way to two lakes. It is located on the border area separating the western part, characterized by hills devoted to the grapevine and olives cultivation, from the eastern side (Northern Apulia region named "Tavoliere"), where wheat is the most common cultivation. Sources of particulate matter could be, apart from the plant emissions, the vehicular traffic from the main road SP10, agricultural activities, and domestic heating. The site is shown in Fig. 1 with a red pin, at the center of a circle with 7 km radius, covering an area of about 154 km^2. Green pins represent the small towns within the area and the orange one indicates the cement plant. About 19,000 inhabitants are residents in this area. The climate is conditioned by the proximity of the Appennino mountains chain and it can be considered as continental, with long cold seasons and short warm seasons. The closest meteorological station is located in Ripacandida, about 2 km away, and it is managed by ALSIA, the regional agency for development and innovation in agriculture. Fig. 2 reports the wind roses for the two seasons (cold, February–April, warm, May–July). These data can be reasonably considered as representative of the measurement site for the closeness of the meteorological station. Moreover, the wind speed and direction measured at the cement plant give similar wind roses (Fig. S1), confirming a quite homogeneous wind field in that area.

It is evident that the prevailing wind direction is South-West and, to a lesser extent, North. Considering the map, some contributions from vehicular traffic is expected. The air masses circulation at the measurement site is described by the back-trajectories cluster analysis, obtained by the HYSPLIT model at NOAA web site (https://www.ready.noaa.gov/HYSPLIT.php), Stein et al. (2015). Fig. 3 shows the clusters for cold and warm periods. In both cases there is a contribution from Atlantic Ocean and North-Europe. The main difference is the contribution of a local trajectory coming from North-Italy in cold season (46%), and from the western Mediterranean area (43%) in the warm season.

3. Instruments and methods

The measurements campaign was carried out using an optical particle sizer (OPS) 3330 TSI and two aethalometers AE33 by MAGEE, and it lasted from 3 February to July 27, 2021. The instruments were located in an open space, close to a big door for loading/unloading of materials at approximately 20 m far from the (CNC) machines and the workbenches for manual products refining. The OPS counts in 16 channels particles, with diameters ranging from 0.3 μm to 10 μm, allowing the estimation of the aerosols number size distributions with a time resolution of 5 min and a flow rate of 2 l/min. Table S1 of the supplementary material shows the OPS channels and the corresponding diameters. The operating principle of the OPS is the detection of radiation scattered by atmospheric particles, as they are sampled by the instrument through a static dissipative flexible tube. No dryer is mounted upstream the instrument. The aethalometers, equipped with a PM2.5 cyclone (M4110 SC Cyclone, Magee Scientific), operate at seven wavelengths (λ = 370, 470, 520, 590, 660, 880, 950 nm). The EBC concentrations are estimated with a time resolution of 1 min and a flow rate of 5 l/min by measuring the light attenuation due to the particles collected on a fiber quartz filter. The cyclones are connected to the aethalometers by means of a static dissipative flexible inlet tube. No dryers are mounted upstream the instruments. Drinovec et al. (2015) improved the aethalometer

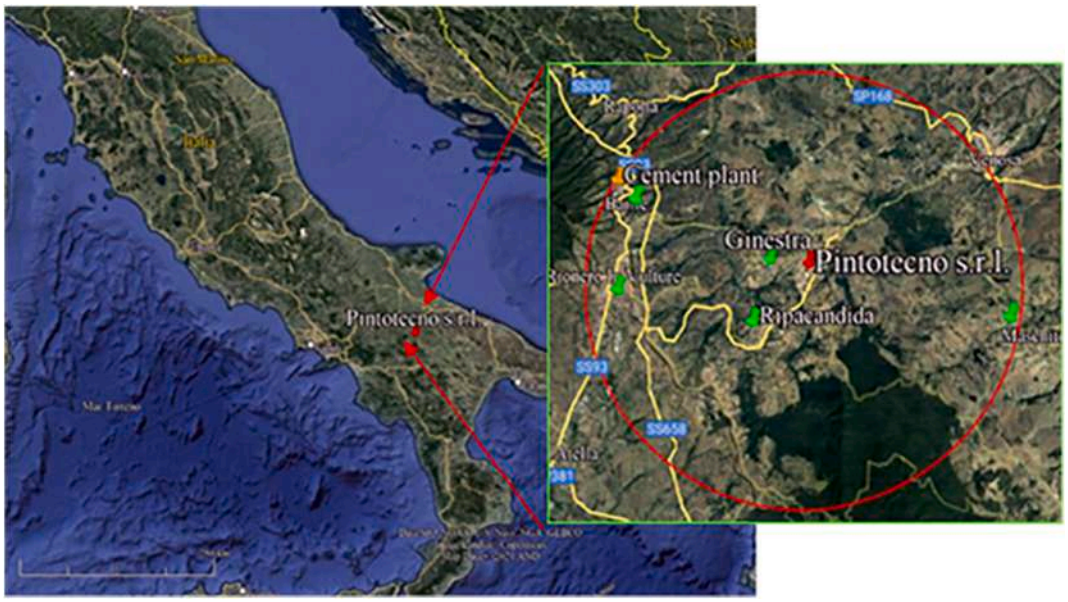

Fig. 1. Measurement site (40.93° N, 15.74° E, 620 m a.s.l.) indicated by a red pin. Green pins indicate the villages within a radius of 7 km far from the site. The orange pin is referred to a cement plant included in the circle.

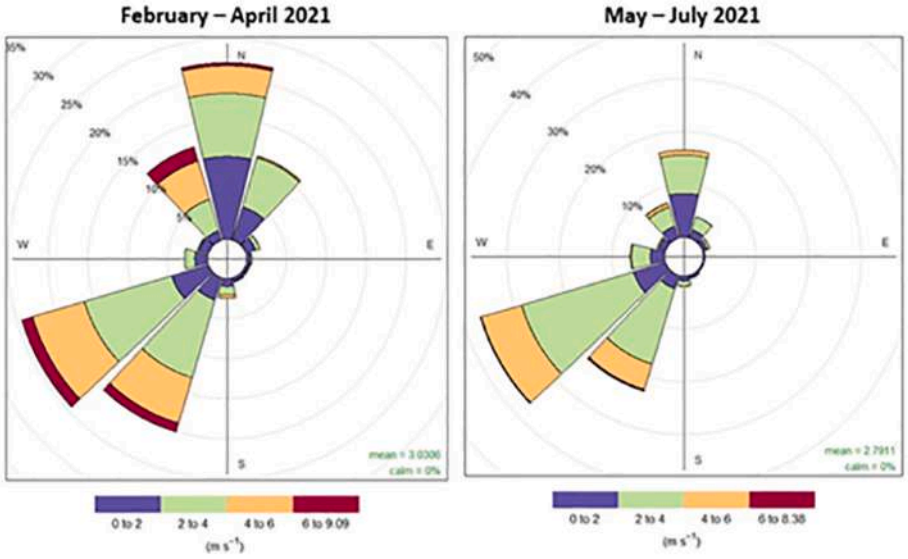

Fig. 2. Wind roses for the cold (February–April) and warm seasons (May–July).

performance with the new version AE33, thanks to the dual spot technology that avoids the shadowing effect. Spectral information on the aerosol absorption coefficients was obtained by means of a best-fit procedure, built to exploit all the 7-wavelengths of the AE33 aethalometer. The absorption coefficient follows, more generally, the Ångström turbidity formula:

$$\sigma_{abs}(\lambda)\alpha(\lambda/\lambda_0)^{-AAE}$$

where σ_{abs} (λ) is the spectral absorption coefficient. The wavelength range of 470–950 nm has been considered to apply the best-fit technique and to estimate AAE parameter since at the UV wavelength there could be some organic compound strongly absorbing with an overestimation of AAE. This allowed distinguishing between incomplete combustion processes such as biomass burning and vehicular traffic. Aethalometers and OPS measurements were averaged on a 1-h time-scale allowing to highlight parameters variation within a single day. Outdoor and indoor EBC measurements lasted for 122 and 150 days respectively, whereas, OPS measured outdoor for 108 days (3 February – 7 June) and indoor for 10 days (9 June – 18 June). Indoor and outdoor EBC measurements led to identifying its outdoor sources, seasonality and influence on both outdoor and indoor aerosol size distributions. Inside OPS measurements lasted a shorter period because the indoor source of particles was strictly related to the manufacturing operations and it was independent from the seasons. The ten-days period of indoor measurement data covered both working and non-working days, and lasted long enough to highlight the differences among particles number size distributions.

The OPS is equipped with a spare internal filter preventing dust deposition on the very sensitive optics of the instrument. A field emission scanning electron microscope (FESEM, Zeiss Supra 40) coupled with an energy-dispersive X-ray spectrometer (EDS, Oxford Inca Energy 350) and an INCA X-act. SDD detector was used to analyze this filter for both outdoor and indoor configurations. Before starting the indoor

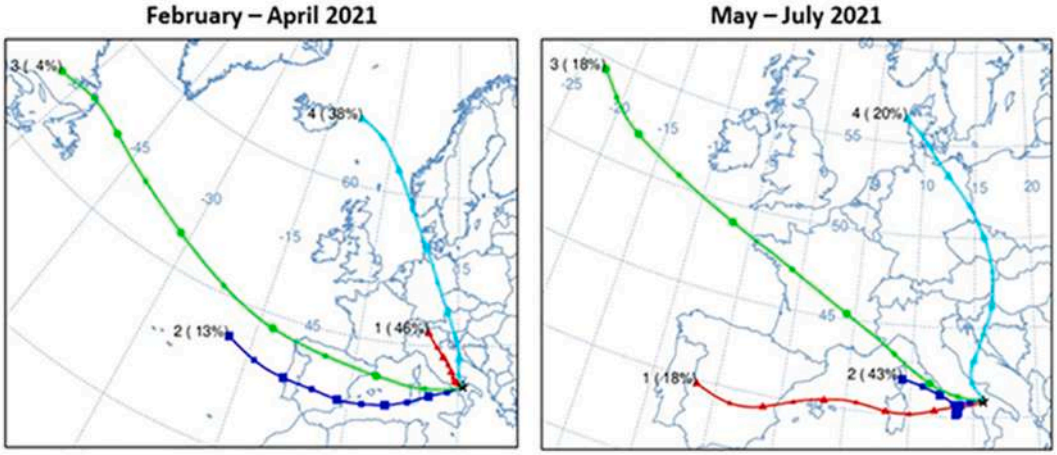

Fig. 3. HYSPLIT back-trajectories clusters for the cold (February–April) and warm seasons (May–July).

campaign, the internal filter was changed. Its fiber structure does not allow a quantitative analysis of the particles trapped on it, but indications on the aerosol morphology and composition can be achieved. The structure of the blank filter is shown in Fig. S2.

4. Results and discussions

4.1. Outdoor and indoor EBC and AAE data

The time behavior of both mean daily outdoor and indoor EBC datasets is shown in Fig. 4. A strong correlation is evident, highlighted by the left scatterplot of 122 simultaneous measurements indoor/outdoor ($R^2 = 0.98$). Undoubtedly, the semi-rural characteristics of the site and the absence of an indoor carbonaceous particles source play a relevant role in obtaining these very high correlations. Polidori et al. (2006) measured indoor and outdoor EC and OC, with a 48-h filter collection time, in 176 homes in urban areas of very big cities in USA and found lower correlations ($R^2 = 0.43$–0.79) for indoor-outdoor EC. Tran et al. (2018) measured, in September 2016, indoor and outdoor EBC at four sites in Hanoi, capital of Vietnam, where the main mode of transport is motorbikes. They found a correlation R = 0.79 which authors considered a high value. For 17 days (19–28 February, 28 May–June 1st, 3–4 June) the AE33s stability was checked in the same indoor configuration, leading to the right scatterplot that shows a very high correlation ($R^2 = 0.998$). However, due to a problem of electrical system at the manufacturing plant, some data were missing from both outdoor and

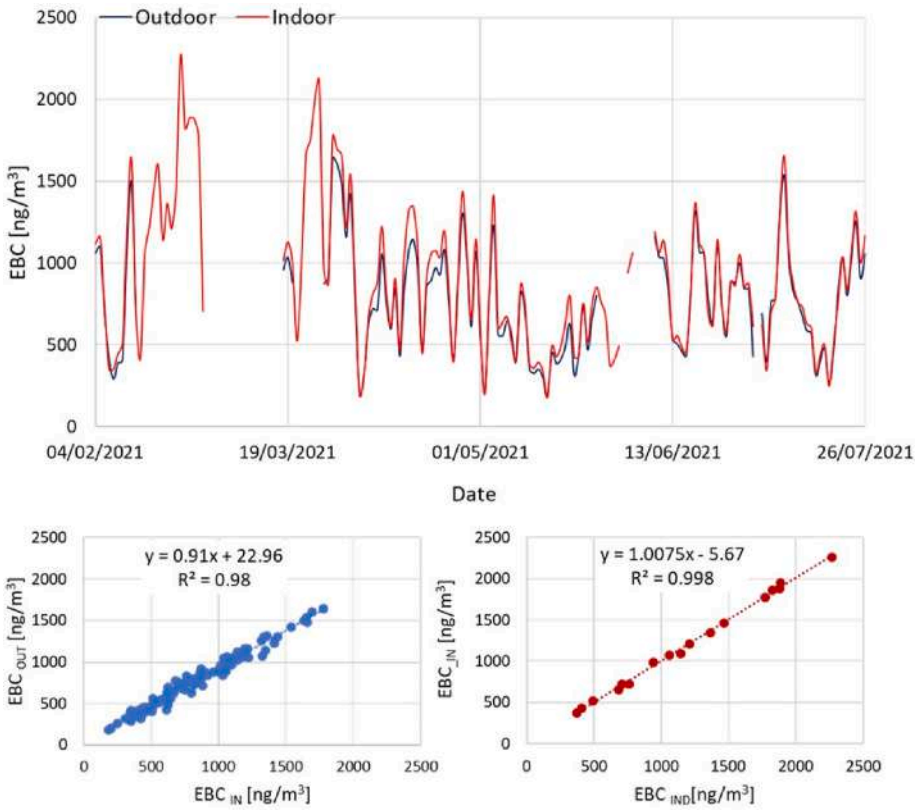

Fig. 4. Indoor and outdoor daily mean EBC time variation. The two scatterplots represent the correlation between the instruments in the outdoor/indoor configuration and in the indoor/indoor configuration, respectively.

indoor AE33s. Excluding the instruments stop, the available days of measurements are 122 and 150 in the outdoor and indoor configurations respectively. Fig. 5a–b shows weekly and diel (working and weekend) cycles of hourly mean EBC concentrations measured outdoor and indoor.

The typical two-peak behavior of EBC daily pattern and the sharp EBC decrease during weekends suggest both the vehicular traffic on the SP10 main road and the vehicles arrival and departure of workers at the Pintotecno plant as one of the sources of carbonaceous particles emission, for both the outdoor and indoor areas. This indicates that outdoor emissions affect indoor air quality through natural ventilation that is by opening and closing big doors during working days, and by infiltration. To our knowledge, no automatic mechanical ventilation system is operating in the plant. This can explain the slightly higher indoor values of EBC than outside ($EBC_{in} = 825 \pm 356$ ng/m^3, $EBC_{out} = 771 \pm 327$ ng/m^3), where wind disperses particles in a more efficient way. As reported by Thatcher et al. (2014), suitable information on the relationship between indoor and outdoor EBC must be looked at for a period long enough to cover the entire emission event. To this aim, since auto vehicular traffic is the main EBC source at the site, the data-set was separated into working days and weekends. The mean EBC_{out} values are 827 ± 455.2 ng/m^3 for working days and 643.8 ± 351.2 ng/m^3 for weekends, whereas the mean EBC_{in} values are 985.2 ± 582.8 ng/m^3 for working days and 707.3 ± 425.5 ng/m^3 for weekends. These mean values lead to an input/output EBC ratio (I/O_{EBC}) equal to 1.07 for the whole data-set, 1.19 for working days and 1.10 for weekends. The EBC ratio (I/O_{EBC}) greater than 1, also during the weekend days, highlights the effect of the entrapment and accumulation of particles inside the plant. Generally, pollutants I/O ratio is found <1, but in the case of Tunno et al. (2015) indoor and outdoor measurements conducted in homes at an industrialized area near Pittsburgh (USA), gave both $PM_{2.5}$ and BC I/O ratios >1, due to the common practice of smoking indoor.

In order to have more information on the possible EBC sources, the polar plot of EBC outdoor concentrations, for the cold and the warm periods are reported (Fig. 6a–b). These plots, obtained by calculating the hourly mean EBC concentrations for wind speed and direction bins, are generally used to have details on the possible pollution sources, as described by Carslaw and Beevers (2013). In this case, the highest concentrations mainly correspond to low wind velocity (2 — 4 m/s) and are observed in the surroundings of the plant, confirming the local vehicular traffic as one of the possible sources. Moreover, in the cold season an EBC hotspot is evident in the Southwestern direction, which is one of the main wind directions for the site and for wind speed equal to 8 m/s. This could correspond both to the main SP10 road (about 600 m far) and to the village of Ripacandida (2 km far, with about 1700 inhabitants). A further contribution to the domestic heating emissions could come from the village of Ginestra (1 km far, with about 700 inhabitants), located in the Northwestern area. The contribution in the Northeastern area could come from the agricultural activities (that is biomass burning of olives branches), confirmed by the lower concentrations observed during the warm season in this sector. In this case, the hotspot is observed for wind speed ≤4 m/s, suggesting only the vehicular traffic on the SP10 main road, closer to the site, as the principal EBC source in the Southwestern direction.

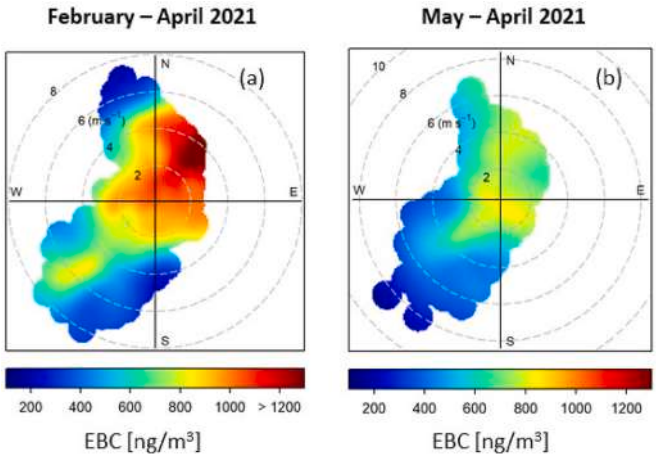

Fig. 6. Outdoor EBC polar plot for the cold (a) and the warm (b) periods.

The indoor and outdoor mean daily AAE time behaviors are shown in

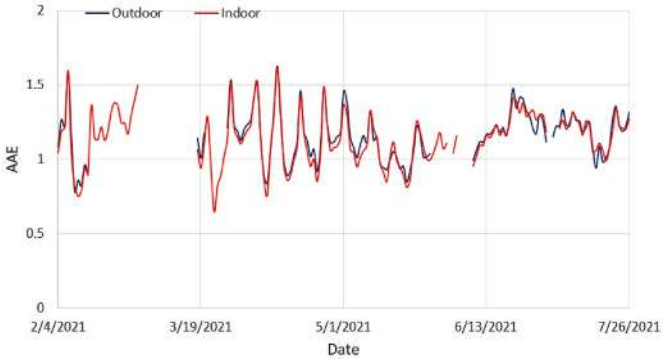

Fig. 7. Indoor and outdoor daily mean AAE time variation.

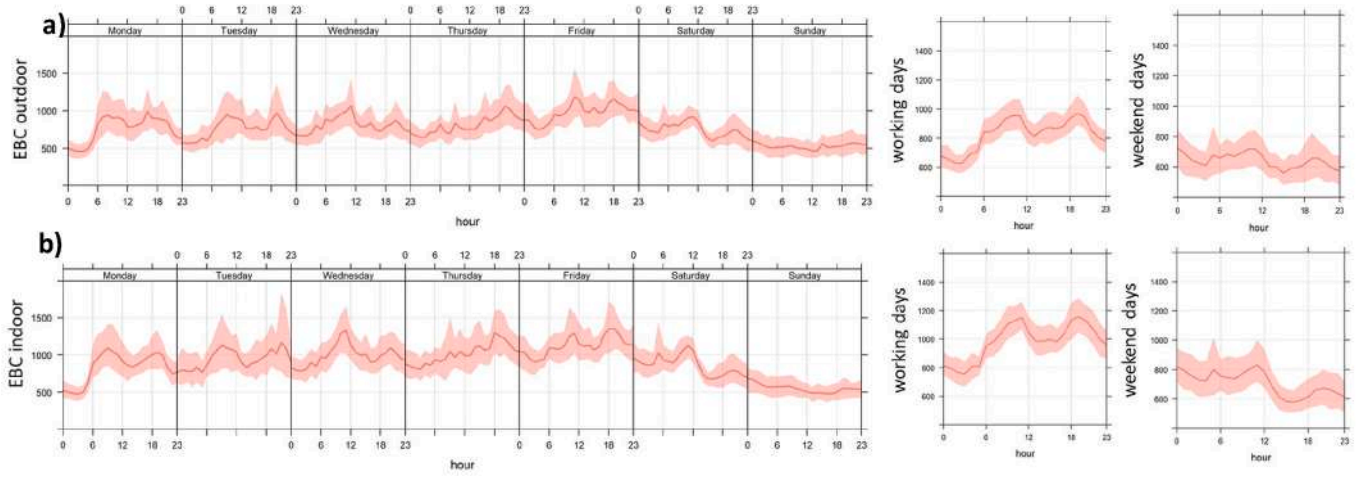

Fig. 5. (a) Weekly and diel (working and weekend) cycles of EBC measured outdoor. (b) The same for EBC measured indoor.

Fig. 7 and, as expected from EBC data comparison, a good agreement is observed.

Average values for the whole period are $AAE_{in} = 1.14 \pm 0.21$ and $AAE_{out} = 1.16 \pm 0.20$, suggesting, outside and inside the plant, the presence of atmospheric particles with similar absorption properties. In particular, the mean values during working days are $AAE_{in} = 1.10 \pm 0.16$ and $AAE_{out} = 1.12 \pm 0.15$, whereas during weekends are $AAE_{in} = 1.24 \pm 0.17$ and $AAE_{out} = 1.24 \pm 0.18$.

The AAE values show higher variations (0.64 — 1.62) in February–April than in May–July with the more intense peaks registered during the cold months suggesting two possible sources of carbonaceous particles. Considering the higher AAE mean values obtained during the weekends, as reported above, one could be the domestic heating, used much more during the weekend when people stay at home. The second could be the burning of vines residues in February and olive branches from March to April, principally during the weekends. These common agricultural operations can be extended until May, due to the longer cold season in this area. The AAE fluctuations tend to reduce in the first summer weeks (0.9 — 1.5) but AAE values remain in the biggest part higher than 1.2 which, in source apportionment studies, is commonly considered as a threshold value to distinguish between traffic-related black carbon and biomass burning (Grange et al., 2020; Kaskaoutis et al., 2021 and references therein). This can be explained by the proximity of the studied area with the Northern Apulia flat region named "Tavoliere", where wheat cultivation, and stubble burning operations after the harvest are widely diffused together with uncontrolled summer fires. In particular, as regards uncontrolled fires, summer 2021 was very hot in "Tavoliere" region, where temperatures as high as 41.8° and 42.3° were recorded in June and July, respectively, by the ARPA Puglia (Puglia Region Environmental Protection Agency) at Foggia meteorological station (http://www.webgis.arpa.puglia.it/meteo/index.php). The temperatures, remaining high for weeks, drying the soil and vegetation, favored the quick expansion of numerous fires that were registered in this period as shown in Fig. 8 from FIRMS satellite based fire products (https://firms.modaps.eosdis.nasa.gov/active_fire/). For the sake of completeness, in the supplementary material a list of links to the websites of local press release fires news is reported.

This continuous source of biomass burning could lead to the accumulation of carbonaceous particles in the boundary layer. In Fig. 9, four NAAPS maps (https://www.nrlmry.navy.mil/aerosol/index_frame.html) showing surface sulfate distributions and smoke concentrations for selected days (June, 13th, June, 23rd, July, 8th, July, 24th) are reported. The maps are obtained from modelling results using AERONET level1.5 data.

Moving from left to right, it is possible to note an increasing smoke surface concentration all over Europe; however local smoke sources can be identified in the area of concern, supporting the idea that the estimated AAE values and their poor variation in June and July can be attributed to the presence of a layer of aged carbonaceous particles.

4.2. Outdoor and indoor number size distributions

As explained previously, the outdoor dataset from the OPS was longer than that of indoor, covering the cold season and, partly, the warm season. This allows identifying outdoor particles sources that can also change according to season. Fig. 10a shows outdoor and indoor mean number size distributions. Outdoor distributions correspond, respectively, to the whole period and to the cold and warm seasons.

Considering the outdoor distributions, it is possible to observe lower values of the mean distribution corresponding to the warm period, especially in the fine fraction. This corroborates the hypothesis of fine particles emissions due to the domestic heating during the cold season, which is not in place in late spring. Moreover, lower ambient temperatures could favor the stability of semi-volatile particles. The highest values of the indoor fine fraction ($D \leq 1$ μm), compared to the outdoor ones suggest a source related to the working operations inside the plant. In Fig. 10b — c, outdoor and indoor mean size distributions for working and non-working days are plotted. In both cases, the shape of the distributions is unchanged but, outside the plant, larger particles fraction increases during the weekend. As stated before, on Saturday and Sunday people staying at home can dedicate time to cultivate their vineyards and olive trees, also by means of agricultural vehicles that favor large particles resuspension. Inside distributions, instead, during non-working days are lower over the whole size range. This result is similar to the outcome obtained by Jensen et al. (2020) that measured, on a one-day measurement campaign, number size distributions during production activities related to 3D printing metal objects. In particular, emptying the 3D printing chamber and spark generation operations lead to higher size distributions than those measured in background conditions. Moreover, it is worth to note that a well-defined mode, centered on 1.56 μm, is present, with similar amplitudes, both indoor and outdoor and independently from the period (cold or warm). Considering that particles with diameter greater than 1 μm are generally produced by mechanical processes (wind soil erosion or mechanical frictions in vehicles), as suggested by Pugatshova et al. (2007), it could be hypothesized that this mode could be associated to the traffic source.

Some more information can be obtained considering the fine fraction named NC_1 (number of particles with $D \leq 1$ μm). Owing to the combustion sources present in the measurements area, a good correlation between EBC and NC_1, especially in the outdoor configuration is

Fig. 8. FIRMS satellite active fires registered for the period June–July 2021. The black pin represents the measurement site.

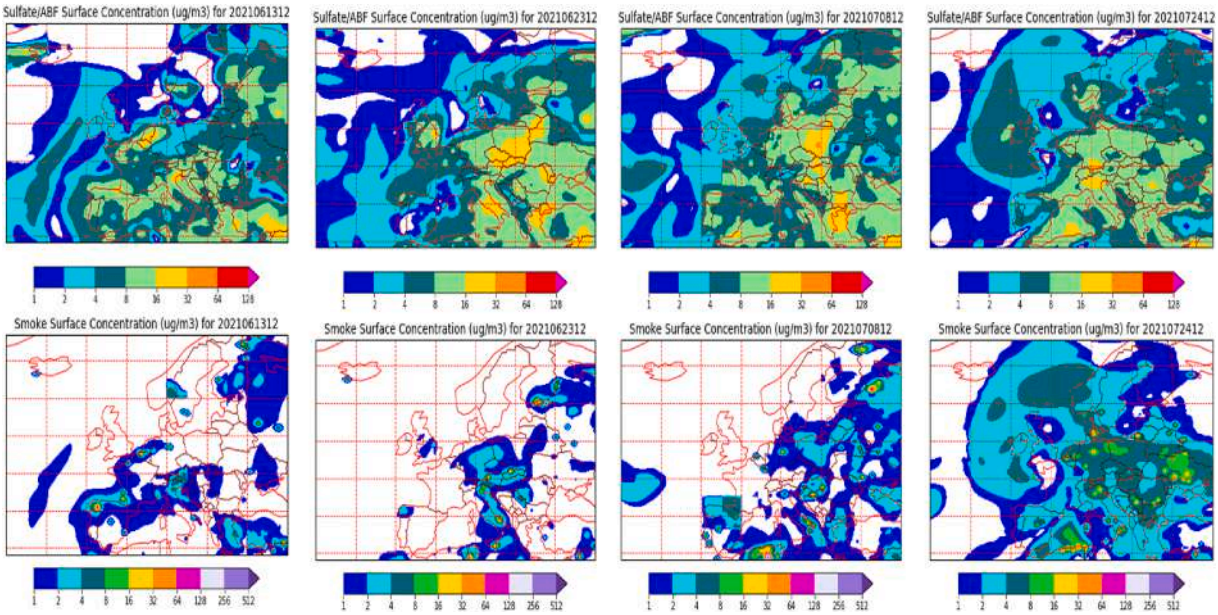

Fig. 9. NAAPS maps of sulfate surface distributions and smoke surface concentrations for four selected days. From left to right, June, 13th, June, 23rd, July, 8th, July, 24th.

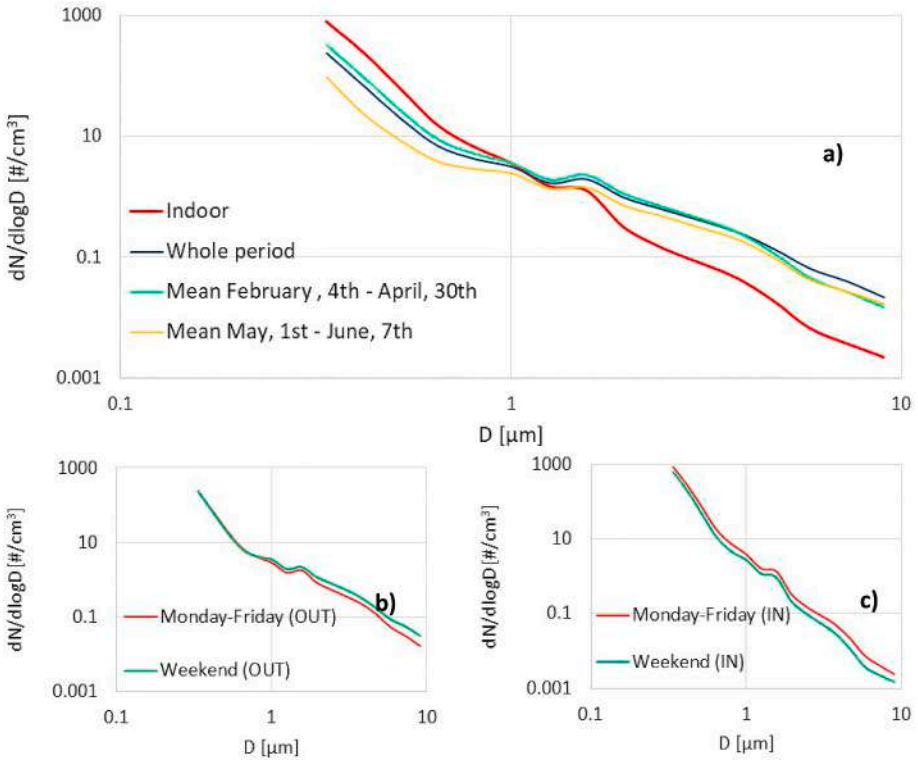

Fig. 10. (a) Mean number size distributions for the outdoor configuration for the whole period, the cold and the warm seasons and for the indoor configuration; (b) Mean number size distributions for outdoor working and non-working days; (c) Mean number size distributions for indoor working and non-working days.

expected: in Fig. 11 the scatterplots of daily mean NC_1 vs. EBC for both the outdoor (left) and indoor (right) conditions are shown. In both cases a correlation can be observed; but the outdoor configuration is higher ($R^2 = 0.69$) than the indoor ($R^2 = 0.57$). Undoubtedly, the external dataset is more rich (75 points) than the internal one (10 points), but these correlations seem to confirm that, outside, carbonaceous particles are important fraction of fine particles.

Fresh fine emitted particles, as BC particles, are more likely found outdoor, due to the closeness to the sources and this could explain the outdoor better correlation shown in Fig. 10. The polar plots of outdoor NC_1 for cold and warm periods, as in Fig. 12, contribute to the characterization of atmospheric particles in the Pintotecno area. It is interesting to note how NC_1 is characterized by higher concentrations in the straight neighborhood of the measurement site and for low wind speed values (2–4 m/s), suggesting activities at the plant as possible sources of the fine fraction particles. As for the EBC (cold period), a hotspot is

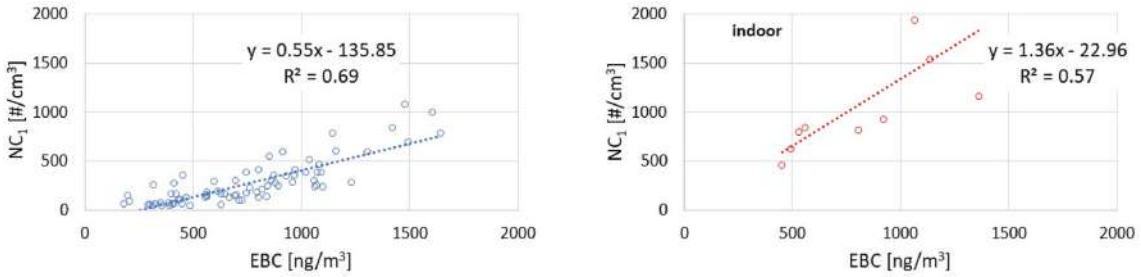

Fig. 11. Scatterplots of daily mean NC1 vs. EBC for the outdoor (left) and indoor (right) conditions.

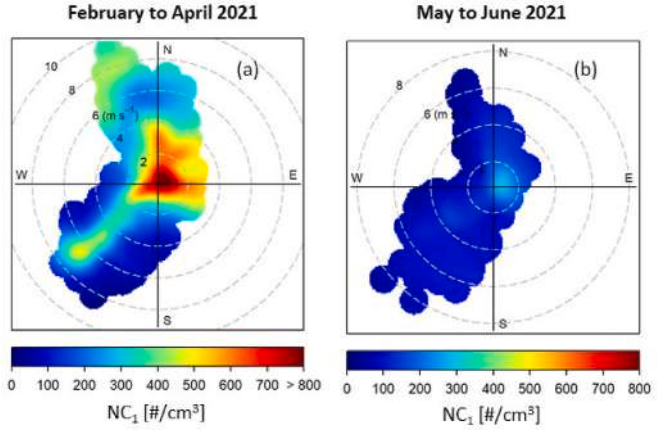

Fig. 12. Outdoor NC_1 polar plot for cold (a) and the warm (b) periods.

located in the South-Western direction, which is the area corresponding to the Ripacandida village and to the prevailing wind directions in cold season. For the sake of completeness, the polar plot corresponding to the warm period (Fig. 12b), is shown, even if the measurements period is shorter (May, 1st – 28) than the corresponding EBC (May–July) and its statistical significance is poor.

4.3. SEM characterization of indoor and outdoor particles

In Fig. 13a and b, a portion of both indoor and outdoor spare filters are shown: metal particles with Zn and Fe–Cr compositions are found. Backscattered electrons images on the right highlight these metal particles, whose presence and composition are naturally related to the specific working operations at the plant. Outdoor Zn-containing particles smaller than indoor Zn particles are observed. Metal particles dimensions can be less than 2 μm (Zn-containing particles) or greater than 2 μm (Fe–Cr particles), but their inhalability raises the question of workers health protection. Indoor/outdoor crustal aluminosilicate particles are also found: as stated above, this is not surprising since quite often big doors are opened and closed to carry workpieces inside the plant and this allows soil particles to enter in the indoor environment. It must be pointed out that, fresh and aged soot particles were found when other areas of the filters were considered; although not shown in these figures. To our knowledge, the present study could be one of the first that has observed particles at a mechanical manufacturing plant, verifying their chemical composition and morphology.

5. Estimation of the potential health risks of EBC

Communicating the pollutants risk exposure to citizens in an appropriate way is more requested. A methodology, proposed by Van der Zee et al.,2016, was applied to express the potential health risk of EBC in terms of equivalent number of passively smoked cigarettes (PSC). The methodology was previously employed in the work by Pavese et al. (2020) for a semi-rural site in South-Italy, hosting the biggest European on-shore pre-treatment plant of crude oil. To this aim, EBC indoor and outdoor mean values measured in the present work over the whole data-set, were converted into daily PSC. As well as in Van der Zee et al. (2016), four health outcomes strictly related to both tobacco smoke and EBC exposure were considered such as low birth weight, decreased lung function, cardiovascular mortality and lung cancer. A number of 2.2 ± 0.6 and 1.9 ± 0.6 PSC was obtained for EBC_{in} and EBC_{out} mean concentration respectively, showing a little higher potential health risk for indoor exposure than for the outdoor. These values were slightly lower compared to the value of 2.8 ± 2.2 calculated at the industrial site of the work of Pavese et al. (2020), but much lower than the value of 11 ± 6 found in March 2016 at an urban center in northern peninsular Southeast Asia (Pani et al., 2020).

6. Conclusions

Outdoor and indoor measurements (February–July 2021) were carried out at a plant of mechanical manufacturing in Southern Italy. In particular, hourly and daily mean number size distributions and EBC concentrations were analyzed to identify aerosol sources at the plant and in the semi-rural area surrounding it. The main results can be summarized as follows:

- 122 days of simultaneous (outdoor and indoor) EBC measurements with a high correlation (0.98) suggests the same sources in both configurations, that is vehicular traffic, domestic heating and agricultural biomass burning for the cold season are the main EBC sources. This result is also supported by the EBC polar plots for cold and warm periods.
- The EBC ratio (I/O_{EBC}) is equal to 1.07 for the whole data-set. Separating these data in working and weekend days, the ratios are 1.19 and 1.10 respectively. This suggests that the absence of an automated ventilation system favor the accumulation of particles coming from the outdoor.
- The AAE values are oscillating (0.64 — 1.62) in February — April with the greatest part of the peaks registered on Sunday. Aside domestic heating, burning of vines residues in February and olive branches from March to April is identified as a local source of the organic component of black carbon. During the warm season, AAE values in the biggest part higher than 1.2, FIRMS active fires and NAAPS maps suggest the influence of a diffuse cloud of aged black carbon due to uncontrolled and prolonged fires in the near "Tavoliere" area (Apulia region).
- The number size distributions have the same shape in both outdoor and indoor configurations. Lower values of the mean outdoor distribution, especially in the fine fraction, correspond to the warm period. This supports the hypothesis of fine particles emissions by domestic heating and agricultural activities during the cold season, not present in the warm one.
- The indoor number fine particles ($D \leq 1$ μm) are characterized by higher values than the outdoor, suggesting a source related to the manufacturing operations inside the plant.

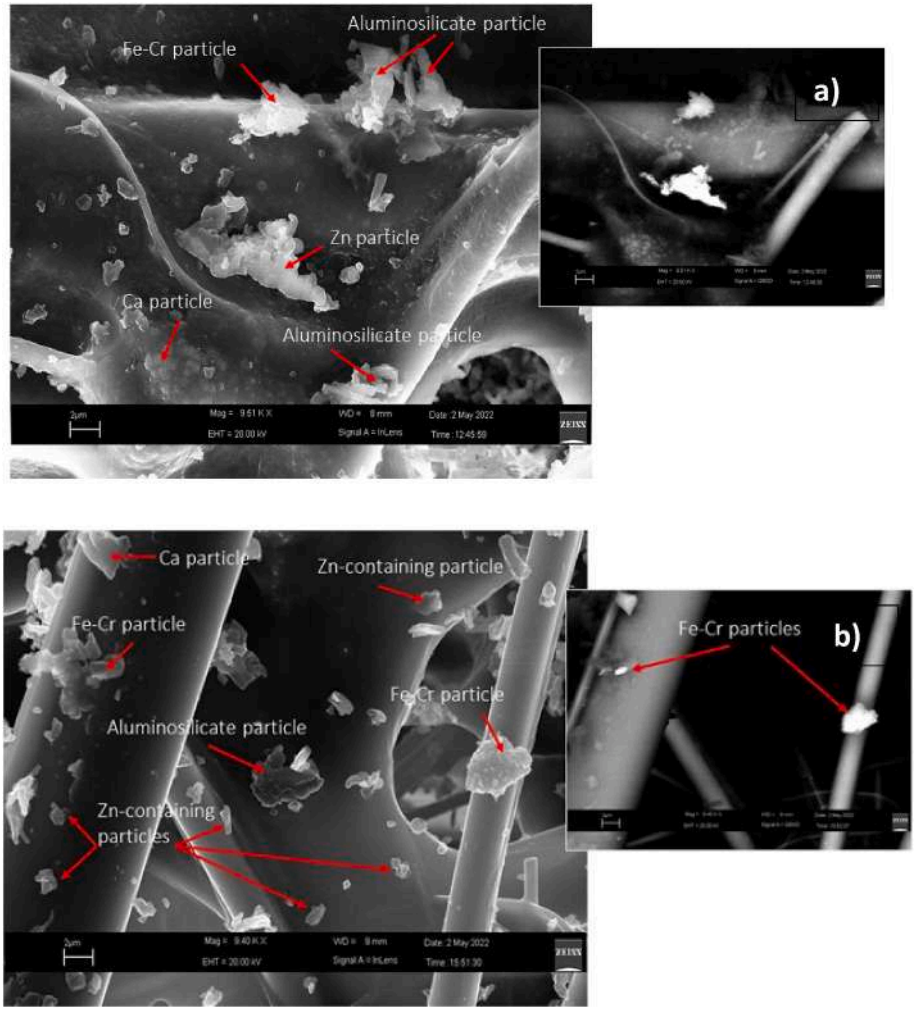

Fig. 13. Indoor (a) and outdoor (b) SEM images, together with backscattered electrons images highlighting metal particles (Fr–Cr and Zn).

- Outdoor fine particles fraction NC_1 ($D \leq 1$ μm) and EBC show a high correlation ($R^2 = 0.69$), whereas indoor data are characterized by a lower one ($R^2 = 0.57$) because moving away from the outdoor traffic source, small fresh carbonaceous particles can easily age and become larger.
- SEM qualitative analysis of the OPS internal spare filter highlights the presence of Zn and Fe–Cr particles, both in indoor and outdoor measurements setup. These particles, can be larger or smaller than 2 μm, and are produced during manual manufacturing operations.
- A methodology, proposed by Van der Zee et al. (2016), was applied to link the number of daily PSC to the measured EBC concentrations. A number of 2.2 ± 0.6 and 1.9 ± 0.6 PSC was obtained for EBC_{in} and EBC_{out} mean concentration respectively, showing a little higher potential health risk for indoor exposure than for the outdoor one.

In conclusion, the synergistic usage of number size distributions and EBC concentrations measurements have proven to be useful to characterize atmospheric particulate in a semi-rural area where a metal manufacturing plant is located. Apart from indoor sources, air quality inside the plant is affected by outdoor aerosol composition and, in some extent, the same happens the other way around. Additional analysis on polycarbonate filters could be useful to definitely assess the aerosol composition and exposure to the pollution of people working at the plant.

CrediT author statement

Giulia Pavese: Conceptualization, Writing – original draft preparation, Funding acquisition and Supervision. Francesca Agresti: Instruments management, Formal analysis. Mariarosaria Calvello: Formal analysis, Writing – original draft preparation. Francesco Esposito: Instruments management, Data curation and analysis. Antonio Lettino: SEM analysis.

Declaration of competing interest

The authors declare that they have no known competing financial interests or personal relationships that could have appeared to influence the work reported in this paper.

Acknowledgements

The Authors appreciate the Italian National Council of Research and Pintotecno s.r.l. for the financial support given for the PhD project “Innovative technologies for the quality of living environment in manufacturing systems” in the framework of cooperation between the Italian National Council of Research and the Italian main Association of Manufacturing and Service Companies. They are also grateful to Dr. Domenico Pinto, COO at PIntotecno; Dr. Renzo Sarli Calace, Logistic & Shopfloor Manager/Innovation Orchestrator; and to Dr. Giuseppe Muscio, R&D Manager for their precious support. The Authors are

thankful to the Agency for Development and Innovation in Agriculture of Basilicata Region for providing meteorological data in Ripacandida and to the Agency for Environmental Protection of Basilicata Region for providing meteorological data at the cement plant in Barile. The NOAA Air Resources Laboratory (ARL) for HYSPLIT model and the NRL/Monterey Aerosol Page for NAAPS maps are acknowledged.

Appendix A. Supplementary data

Supplementary data to this article can be found online at https://doi.org/10.1016/j.apr.2022.101488.

References

Bhanarkar, A.D., Majumdar, D., Nema, P., George, K.V., 2010. Emissions of SO2, NOx and particulates from a pipe manufacturing plant and prediction of impact on air quality. Environ. Monit. Assess. 169, 677–685. https://doi.org/10.1007/s10661-009-1207-z.

Cartechini, L., et al., 2015. Acute episodes of black carbon and aerosol contamination in a museum environment: results of integrated real-time and off-line measurements. Atmos. Environ. 116, 130–137. https://doi.org/10.1016/j.atmosenv.2015.06.033.

Carslaw, D.C., Beevers, S.D., 2013. Characterising and understanding emission sources using bivariate polar plots and k-means clustering. Environ. Model. Software 40, 325–329. https://doi.org/10.1016/j.envsoft.2012.09.005.

Chen, R., et al., 2020. Exposure, assessment and health hazards of particulate matter in metal additive manufacturing: a review. Chemosphere 259, 127452. https://doi.org/10.1016/j.chemosphere.2020.127452.

Conner, T.L., Norris, G.A., Landis, M.S., Williams, R.W., 2001. Individual particle analysis of indoor, outdoor, and community samples from the 1998 Baltimore particulate matter study. Atmos. Environ. 35, 3935–3946. https://doi.org/10.1016/S1352-2310(01)00191-1.

Drinovec, L., et al., 2015. The "dual-spot" Aethalometer: an improved measurement of aerosol black carbon with real-time loading compensation. Atmos. Meas. Tech. 8, 1965–1979. https://doi.org/10.5194/amt-8-1965-2015.

Ehrlich, C., et al., 2007. PM10, PM2.5 and PM1.0—emissions from industrial plants—results from measurement programmes in Germany. Atmos. Environ. 41, 6236–6254. https://doi.org/10.1016/j.atmosenv.2007.03.059.

Grange, S.K., Lötscher, H., Fischer, A., Emmenegger, L., Hueglin, C., 2020. Evaluation of equivalent black carbon source apportionment using observations from Switzerland between 2008 and 2018. Atmos. Meas. Tech. 13, 1867–1885. https://doi.org/10.5194/amt-13-1867-2020.

Jensen, A.C.Ø., Harboe, H., Brostrøm, A., Jensen, K.A., Fonseca, A.S., 2020. Nanoparticle exposure and workplace measurements during processes related to 3D printing of a metal object. Front. Public Health 8, 608718. https://doi.org/10.3389/fpubh.2020.608718.

Jones, A.M., Harrison, R.M., 2016. Emission of ultrafine particles from the incineration of municipal solid waste: a review. Atmos. Environ. 140, 519–528. https://doi.org/10.1016/j.atmosenv.2016.06.005.

Kaskaoutis, D.G., Grivas, G., Stavroulas, I., Bougiatioti, A., Liakakou, E., Dumka, U.C., Gerasopoulos, E., Mihalopoulos, N., 2021. Apportionment of black and brown carbon spectral absorption sources in the urban environment of Athens, Greece, during winter. Sci. Total Environ. 801 (2021), 149739. https://doi.org/10.1016/j.scitotenv.2021.149739.

Küpper, M., et al., 2018. Contributions of carbonaceous particles from fossil emissions and biomass burning to PM10 in the Ruhr area, Germany. Atmos. Environ. 189, 174–186. https://doi.org/10.1016/j.atmosenv.2018.06.039.

Leung, D.Y.C., 2015. Outdoor-indoor air pollution in urban environment: 547 challenges and opportunity. Front. Environ. Sci. https://doi.org/10.3389/fenvs.2014.00069.

Moon, K.J., et al., 2008. Source apportionment of fine carbonaceous particles by positive matrix factorization at Gosan background site in East Asia. Environ. Int. 34, 654–664. https://doi.org/10.1016/j.envint.2007.12.021.

Nezis, I., et al., 2022. Linking indoor particulate matter and black carbon with sick building syndrome symptoms in a public office building. Atmos. Pollut. Res. 13, 101292 https://doi.org/10.1016/j.apr.2021.101292.

Noth, E.M., et al., 2014. Hammond Development of a job-exposure matrix for exposure to total and fine particulate matter in the aluminum industry. J. Expo. Sci. Environ. Epidemiol. 24 (1), 89–99. https://doi.org/10.1038/jes.2013.53.

Pani, S.K., Wang, S.H., Lin, N.H., Chantara, S., Lee, C.T., Thepnuan, D., 2020. Black carbon over an urban atmosphere in northern peninsular Southeast Asia: characteristics, source apportionment, and associated health risks. Environ. Pollut. 259, 113871 https://doi.org/10.1016/j.envpol.2019.113871.

Pavese, G., Calvello, M., Castagna, J., Esposito, F., 2020. Black carbon and its impact on air quality in two semi-rural sites in Southern Italy near an oil pre-treatment plant. Atmos. Environ. 233, 117532 https://doi.org/10.1016/j.atmosenv.2020.117532.

Polidori, A., et al., 2006. Fine organic particulate matter dominates indoor-generated PM2.5 in RIOPA homes. J. Expo. Sci. Environ. Epidemiol. 16, 321–331. https://doi.org/10.1038/sj.jes.7500476.

Pugatshova, A., Reinart, A., Tamm, E., 2007. Features of the multimodal aerosol size distribution depending on the air mass origin in the Baltic region. Atmos. Environ. 41 (21), 4408–4422. https://doi.org/10.1016/j.atmosenv.2007.01.044.

Riffault, V., et al., 2015. Fine and ultrafine particles in the vicinity of industrial activities: a review. Crit. Rev. Environ. Sci. Technol. 45 (21), 2305–2356. https://doi.org/10.1080/10643389.2015.1025636.

Singh, A., et al., 2017. Indoor air pollution and its association with poor lung function, microalbuminuria and variations in blood pressure among kitchen workers in India: a cross-sectional study. Environ. Health 16, 33. https://doi.org/10.1186/s12940-017-0243-3.

Stefaniak, A.B., Du Preez, S., Du Plessis, J.L., 2021. Additive manufacturing for occupational hygiene: a comprehensive review of processes, emissions, & exposures. J. Toxicol. Environ. Health, Part B 24 (5), 173–222. https://doi.org/10.1080/10937404.2021.1936319.

Stein, A.F., et al., 2015. NOAA's HYSPLIT atmospheric transport and dispersion modeling system. Bull. Am. Meteorol. Soc. 96, 2059–2077. https://doi.org/10.1175/BAMS-D-14-00110.1.

Thatcher, T.L., Kirchstetter, T.W., Malejan, C.J., Ward, C.E., 2014. Infiltration of black carbon particles from residential woodsmoke into nearby homes. Open J. Air Pollut. 3, 111–120. https://doi.org/10.4236/ojap.2014.34011.

Tran, L.K., Quang, N., Hue, N.T., Dat, M.V., Morawska, L., Nieuwenhuijsen, M., Thai, P. K., 2018. Exploratory assessment of outdoor and indoor airborne black carbon in different locations of Hanoi Vietnam. Sci. Total Environ. 642, 1233–1241. https://doi.org/10.1016/j.scitotenv.2018.06.146.

Tunno, B.J., Naumoff Shields, K., Cambal, L., Tripathy, S., Holguin, F., Lioy, P., Clougherty, J.E., 2015. Indoor air sampling for fine particulate matter and black carbon in industrial communities in Pittsburgh. Sci. Total Environ. 536, 108–115. https://doi.org/10.1016/j.scitotenv.2015.06.117.

van der Zee, S.C., Fischer, P.H., Hoek, G., 2016. Air pollution in perspective: health risks of air pollution expressed in equivalent numbers of passively smoked cigarettes. Environ. Res. 148, 475–483. https://doi.org/10.1016/j.envres.2016.04.001.